PHYSICAL REVIEW D **73,** 023009 (2006)

Reduced shear power spectrum

Scott Dodelson,[1,2,3] Charles Shapiro,[4,5] and Martin White[6,7]

[1]*NASA/Fermilab Astrophysics Center, Fermi National Accelerator Laboratory, Batavia, Illinois 60510-0500, USA*
[2]*Department of Astronomy & Astrophysics, The University of Chicago, Chicago, Illinois 60637-1433, USA*
[3]*Department of Physics and Astronomy, Northwestern University, Evanston, Illinois 60208, USA*
[4]*Department of Physics, The University of Chicago, Chicago, Illinois 60637-1433, USA*
[5]*Kavli Institute for Cosmological Physics, The University of Chicago, Chicago, Illinois 60637-1433, USA*
[6]*Department of Astronomy, University of California, Berkeley, California 94720, USA*
[7]*Department of Physics, University of California, Berkeley, California 94720, USA*

(Received 2 September 2005; published 31 January 2006)

Measurements of ellipticities of background galaxies are sensitive to the *reduced shear*, the cosmic shear divided by $(1 - \kappa)$ where κ is the projected density field. We compute the difference between shear and reduced shear both analytically and with simulations. The difference becomes more important on smaller scales, and will impact cosmological parameter estimation from upcoming experiments. A simple recipe is presented to carry out the required correction.

DOI: 10.1103/PhysRevD.73.023009 PACS numbers: 98.62.Sb, 98.80.−k

I. INTRODUCTION

One of the most fascinating aspects of general relativity, and the first triumph for the theory, is that gravitational potentials can act as lenses for light from distant sources. The presence of large-scale structure and its associated potentials along the line-of-sight to distant galaxies implies that the images of most distant galaxies are slightly sheared compared to their intrinsic shapes. This shearing effect encodes information about cosmological distances and the evolution of large-scale structure. For this reason gravitational lensing of background galaxies by large-scale structure (cosmic shear) offers an excellent way to study the distribution of matter in the universe [1–4]. Measurements of the cosmic shear are already enabling us to constrain the dark matter abundance and clustering amplitude among other parameters [5–8]. In the future, large surveys may well uncover properties of dark energy, such as its abundance and equation of state [9–12], and of neutrinos [13,14]. This program will be successful only if we can make very accurate theoretical predictions [15].

As experiments begin to go deeper and cover more and more sky, theorists must make sure that predictions are accurate enough to extract cosmological information in an unbiased fashion. There is a quantitative way to phrase this directive: the systematic errors on cosmological parameters induced by theoretical uncertainties should be significantly smaller than the anticipated statistical errors. Since the latter hover near the percent level for the most ambitious experiments, theorists clearly have their work cut out for them.

Here we consider one correction to the standard theoretical predictions, the effect of reduced shear [16–18]. The observed ellipticities of galaxies (with two components g_i for each galaxy) are often used as estimates of the cosmic shear (γ_i), but in fact they are sensitive to the reduced shear:

$$g_i = \frac{\gamma_i}{1 - \kappa}, \qquad |\kappa| < 1 \tag{1}$$

where κ is the convergence or roughly the projected density field. We analyze the difference between shear and reduced shear both analytically and with numerical simulations [19,20], focusing on various two-point functions. Then we map out the region in experiment-space where the effects of reduced shear need to be included. Outside of this region, the canonical prediction—which neglects the $1 - \kappa$ denominator—is sufficient.

Throughout we assume a flat, ΛCDM cosmology. Our base model has $\Omega_m = 0.28$, $\Omega_b h^2 = 0.024$, $h = 0.7$, $n = 1$, and $\sigma_8 = 0.9$. We will let the galaxy density and sky coverage of surveys vary, but we limit ourselves to all background sources at $z = 1$. Our quantitative results will change slightly for higher redshift sources, but our two major conclusions—that we can compute these corrections accurately and that we have to compute them if we want to extract cosmological parameters—are only strengthened (since the effect is larger) for higher redshift sources.

II. SHEAR TWO-POINT FUNCTIONS

Here we briefly review a variety of definitions relating to cosmic shear and its statistics. Cosmic shear can be represented by two numbers at any point in space, γ_1 and γ_2. Similarly, the ellipticity of a background galaxy can be described by g_1 and g_2. The latter are measurable, while the former are related in a straighforward way to the projected gravitational potential and therefore are simplest to compute given a cosmological theory. On average, all these components are zero; however their two-point functions contain information about cosmic fluctuations.

We focus here on four sets of two-point functions, each of which can be expressed as an integral over the 3D power spectrum with different weightings.

 © 2006 The American Physical Society

(i) *Smoothed Variance* Defining $\gamma \equiv \gamma_1 + i\gamma_2$, make a map of γ smoothed over a square pixel of side θ. The variance of the smoothed shear field, $\bar{\gamma}$, is then

$$\langle|\bar{\gamma}|^2\rangle(\theta) = \langle\bar{\gamma}_1^2\rangle(\theta) + \langle\bar{\gamma}_2^2\rangle(\theta) \tag{2}$$

with a similar definition for the galaxy ellipticities, g. Note that "$^-$" denotes an average over a local square while angle brackets denote an average over the sky.

(ii) *Aperture Mass* At any sky position θ_0, this is a 2D integral over the *tangential shear*, $\gamma_t \equiv -\gamma_1\cos(2\phi) - \gamma_2\sin(2\phi)$, where ϕ is the angle between θ_0 and a fixed x-axis. The weighting function in the integral depends on a smoothing scale θ. Here we use the smoothing function defined in [16]. The average value of $M_{\rm ap}$ is zero, but its variance as a function of smoothing scale contains information about the underlying fluctuations.

(iii) *Correlation Function* Since there are two components of shear, there are in principle 3 separate correlation functions $\langle\gamma_i(\theta_0)\gamma_j(\theta_0+\theta)\rangle$ averaged over all positions θ_0. These depend on the angular difference $\theta \equiv |\theta|$. Here we focus on the combination $\xi(\theta) \equiv \langle\gamma(\theta_0)\gamma^*(\theta_0+\theta)\rangle$.

(iv) *Angular Power Spectrum* Write the γ_i field as a sum of coefficients times spherical harmonics. In the small angle limit in which we will work, this is equivalent to a Fourier transform, $\tilde{\gamma}_i(\boldsymbol{l})$. One linear combination of these Fourier coefficients (the so-called "B-mode") vanishes if the underlying fluctuations are due to scalar perturbations; the other,

$$\tilde{E}(\boldsymbol{l}) = \epsilon_{ij}T_i(\boldsymbol{l})\tilde{\gamma}_j(\boldsymbol{l}), \tag{3}$$

is sensitive to the projected gravitational potential. Here ϵ_{ij} is the 2D antisymmetric tensor $\epsilon_{12} = -\epsilon_{21} = 1$; and the trigonometric weighting functions are

$$T_1(\boldsymbol{l}) \equiv -\sin(2\phi_l) \qquad T_2(\mathbf{l}) \equiv \cos(2\phi_l) \tag{4}$$

where ϕ_l is the angle of $\boldsymbol{l}$ with a fixed x-axis. The angular power spectrum is roughly the variance of these Fourier coefficents,

$$\langle\tilde{E}(\boldsymbol{l})\tilde{E}(\boldsymbol{l}')\rangle = (2\pi)^2\delta^2(\boldsymbol{l}+\boldsymbol{l}')C_l. \tag{5}$$

Each of these two-point functions can be computed from a simulation using either shear or reduced shear. Thus, for example, we can measure in a simulation both C_l^γ and C_l^g and find the difference between the two. The simulations we use to compute these functions are described in Ref. [18]. We can also compute the two-point functions semianalytically. The two-point functions of γ can be expressed in terms of integrals over the 3D matter power spectrum, which has been extremely well-studied [21–25]. The two-point functions of g can be computed perturbatively by expanding the $1-\kappa$ denominator around $\kappa = 0$. In Sec. III, we write the shear two-point functions as integrals of the 3D matter power spectrum (these expressions are well-known [1,4]) and the reduced shear corrections in terms of the 3D three-point function, the matter bispectrum.

III. PERTURBATIVE CALCULATION

The simplest two-point function to compute is the angular power spectrum. The Fourier transformed shear can be expressed in terms of the projected gravitational potential

$$\tilde{\gamma}_i(\boldsymbol{l}) = -\epsilon_{ij}T_j(\boldsymbol{l})\frac{l^2}{2}\tilde{\psi}(\mathbf{l}) \tag{6}$$

with

$$\tilde{\psi}(\boldsymbol{l}) \equiv \int_0^\infty \frac{d\chi}{\chi}W(\chi)\int\frac{dk_3}{2\pi}\tilde{\Phi}(\boldsymbol{l}/\chi, k_3;\chi). \tag{7}$$

Here χ is comoving distance; the lensing kernel $W = 2\chi(1-\chi/\chi_s)\Theta(\chi_s-\chi)$ with χ_s the distance to the source galaxy and Θ the Heaviside step function.

Inserting Eq. (6) into Eq. (3) to get $\tilde{E}(\boldsymbol{l})$, multiplying $\tilde{E}(\boldsymbol{l})$ by $\tilde{E}(\boldsymbol{l})'$, taking the expectation value, and then integrating over $\boldsymbol{l}'$ in the Limber approximation leads to

$$C_l = \frac{l^4}{4}\int\frac{d\chi W^2(\chi)}{\chi^6}P_\Phi(l/\chi;\chi) \tag{8}$$

where P_Φ is the 3D power spectrum of the gravitational

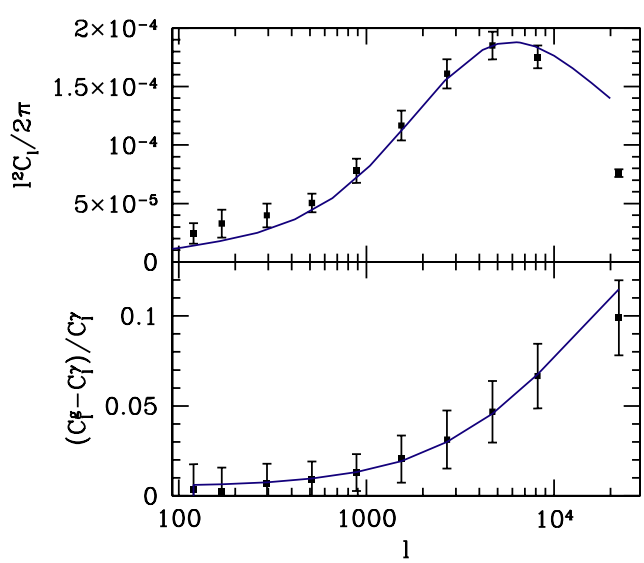

FIG. 1 (color online). Results from simulations (points with error bars) and the perturbative calculation (smooth curves) for the zero order power spectrum (top panel) and the fractional change due to reduced shear (bottom panel). The error bars are estimates of sample variance [18] and are not intended to illustrate the agreement with the semianalytic result.

potential. The top panel of Fig. 1 shows the power spectrum computed in this fashion as compared with that measured in simulations. Agreement is excellent, confirming earlier work [26,27]. The one aberrant point on small scales in the simulations is close to the Nyquist frequency, so power in the simulation is artifically suppressed.

Equation (8) is an expression for the power spectrum of cosmic shear, C_l^γ. To lowest order, when $\kappa \to 0$ in Eq. (1), the power spectrum of the observable reduced shear is equal to this. We can perturbatively compute the correction to the reduced shear: to leading order, $g^{(1)} = \gamma$ and to second order $g^{(2)} = \gamma\kappa$. Therefore, the correction to the two-point function due to reduced shear is

$$\delta\langle\tilde{E}(\boldsymbol{l})\tilde{E}(\boldsymbol{l}')\rangle = \epsilon_{ij}\epsilon_{kl}T_i(\boldsymbol{l})T_k(\boldsymbol{l}')\langle\tilde{g}_j^{(2)}(\boldsymbol{l})\tilde{g}_l^{(1)}(\boldsymbol{l}')\rangle + (\boldsymbol{l}\leftrightarrow\boldsymbol{l}') \tag{9}$$

Plugging in for $\tilde{E}$ and using $\epsilon_{ij}\epsilon_{jk} = -\delta_{ik}$, we have

$$\delta\langle\tilde{E}(\boldsymbol{l})\tilde{E}(\boldsymbol{l}')\rangle = \frac{-l^2}{8}T_i(\boldsymbol{l})\int\frac{d^2l_1}{(2\pi)^2}T_i(\boldsymbol{l}_1)l_1^2(\boldsymbol{l}-\boldsymbol{l}_1)^2 \times\langle\tilde{\psi}(\boldsymbol{l}_1)\tilde{\psi}(\boldsymbol{l}-\boldsymbol{l}_1)\tilde{\psi}(\boldsymbol{l}')\rangle + (\boldsymbol{l}\leftrightarrow\boldsymbol{l}') \tag{10}$$

Using Eqs. (19), (20) and (22) in Ref. [28], we can reduce this to

$$\delta C_l = \frac{2T_i(l)}{l^4}\int\frac{d^2l_1}{(2\pi)^2}T_i(\mathbf{l}_1)l_1^2(\boldsymbol{l}-\boldsymbol{l}_1)^2B^\kappa(\boldsymbol{l}_1,\boldsymbol{l}-\boldsymbol{l}_1,-\boldsymbol{l}) \tag{11}$$

where B^κ is the bispectrum of the convergence. Just as the power spectrum of the convergence can be written as an integral of the 3D power spectrum along the line-of-sight (Eq. (8)), the 2D bispectrum is an integral of the 3D bispectrum [29]:

$$B^\kappa(\boldsymbol{l}_1,\boldsymbol{l}_2,\boldsymbol{l}_3) = \frac{-l^6}{8} \times\int_0^\infty d\chi\frac{W^3(\chi)}{\chi^{10}}B_\Phi(\boldsymbol{l}_1/\chi,\boldsymbol{l}_2/\chi,\boldsymbol{l}_3/\chi). \tag{12}$$

The 3D bispectrum, B_Φ, has been computed analytically on large scales and measured on a wide range of scales in simulations [24]. An accurate fit to the N-body results was introduced in Ref. [30]; we use this fit to compute δC_l, the difference between cosmic shear and reduced shear power. The power spectrum, P_Φ, which is needed to compute B_Φ, was computed using the publicly available Halofit code [25] which has also been calibrated by numerical simulations. Figure 1 shows the results of this perturbative calculation and of a similar measurement from simulations. The perturbative results are in excellent agreement with the simulations. This is extremely encouraging because it offers an easy way to include reduced shear corrections without resorting to expensive simulations.

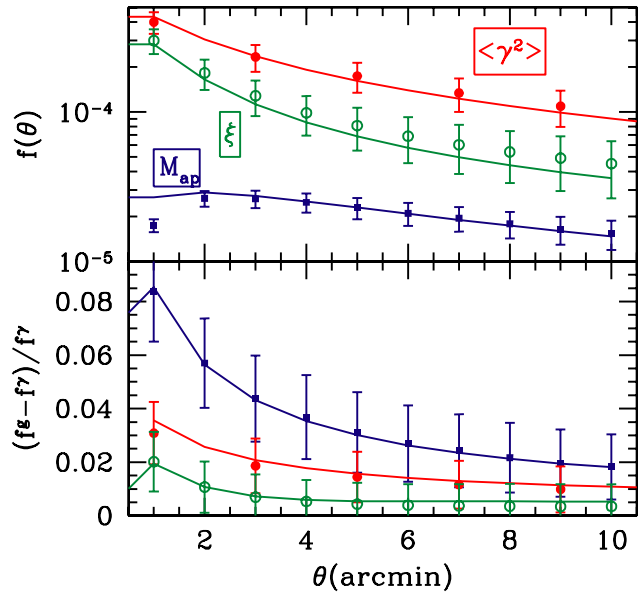

FIG. 2 (color online). Angular two-point functions from simulations and perturbatively. The error bars are estimates of sample variance [18] and are not intended to illustrate the agreement with the semianalytic result.

The conclusion that reduced shear differs from cosmic shear most significantly on small scales follows from perturbation theory. On large scales, fluctuations in γ and κ are small; since the difference between cosmic shear and reduced shear is higher order in these perturbations ($\propto \kappa\gamma$), it is very small on large scales.

The angular two-point functions described in §II can all be expressed as integrals over the power spectrum. The smoothed variance is

$$\langle|\bar{\gamma}^2|\rangle(\theta) = \frac{1}{\pi^2}\int d^2l\tilde{j}_0(l_1\theta/2)j_0(l_2\theta/2)C_l. \tag{13}$$

This variance can be computed for either shear or reduced shear. The difference between the two is the same integral over δC_l from Eq. (11). The other spatial functions are

$$\langle M_{\rm ap}^2\rangle(\theta) = \frac{288}{\pi\theta^4}\int_0^\infty dl\frac{C_lJ_4^2(l\theta)}{l^3} \tag{14}$$

and

$$\xi(\theta) = \frac{1}{2\pi}\int_0^\infty dl\ lJ_0(l\theta)C_l. \tag{15}$$

We have computed these three functions from simulations and perturbatively; the results are shown in Fig. 2. The simulations and perturbative calculations agree extremely well, as do the corrections.

IV. IMPACT ON COSMOLOGICAL PARAMETERS

When does one need to include the effects of reduced shear when comparing models with observations?

Neglecting these effects results in an incorrect prediction for the power spectrum; we computed a correction, δC_l, above. This incorrect prediction propagates to an incorrect estimate of the cosmological parameters, p_i, or a bias. The bias on parameter i is

$$b_i \equiv p_i^{\rm true} - p_i = F_{ij}^{-1} \sum_l w_l \frac{\partial C_l}{\partial p_j} \delta C_l. \tag{16}$$

Here w_l is the weight, the inverse variance of the measurement, and F is the Fisher matrix

$$F_{ij} = \sum_l w_l \frac{\partial C_l}{\partial p_i} \frac{\partial C_l}{\partial p_j}. \tag{17}$$

The variance depends on experimental specifications: sky coverage and depth/resolution. Specifically,

$$w_l^{-1} = \frac{2}{(2l+1) f_{\rm sky}} \left(C_l + \frac{\langle \gamma_{\rm int}^2 \rangle}{n_{\rm eff}} \right). \tag{18}$$

The fraction of sky covered is $f_{\rm sky}$, while the rms of the intrinsic ellipticity of galaxies, $\langle \gamma_{\rm int}^2 \rangle^{1/2}$, is set to 0.25 [10,31], and $n_{\rm eff}$ is the effective galaxy density which depends mainly on the depth and resolution of the experiment.

We can compute the bias induced by neglecting the difference between shear and cosmic shear for any experiment. For concreteness, we allow three cosmological parameters to vary: the normalization of the power spectrum, σ_8; the shape of the power spectrum, $\Gamma \simeq \Omega_m h$; and the matter density, Ω_m. Figure 3 shows the bias induced in these parameters by neglected the cosmic shear corrections. This bias was computed including data out to $l = 3000$. The cut-off is necessary because baryons affect the theoretical predictions on small scales [32,33], and it is very difficult to predict these effects accurately.

Since the reduced shear corrections on scales $l < 3000$ are of order a few percent (Fig. 1), it is not surprising that the induced biases on the parameters are also of order a few percent. Note from Eq. (16) that the bias scales as $F^{-1} w_l$. Since $w_l \propto f_{\rm sky}^{-1}$, and F^{-1} scales as $f_{\rm sky}$ the bias is nearly independent of sky coverage. Therefore, the bias depends only on the galaxy density. At very large density, the weight w_l becomes independent of galaxy density, since shape noise due to intrinsic ellipticity is inversely proportional to galaxy density. In this limit, cosmic variance—the first term in parentheses in Eq. (18)—becomes the dominant source of noise. The largest bias is to the normalization parameter σ_8.

How important is a one to 2% level bias in the cosmological parameters? We must compare the bias to the anticipated statistical error in an experiment. With only one free parameter, this comparison is straightforward: a bias should not be greater than the uncertainty in the parameter. Figure 4 shows the ratio of bias to statistical error for the most severely affected cosmological parameter (σ_8) as a function of survey width ($f_{\rm sky}$) and galaxy density. We use the unmarginalized error, meaning that we consider all other parameters fixed.

With several parameters allowed to vary, we use an analogous touchstone: a bias must not cause the estimated parameters to lie outside of the 1-σ error ellipsoid in parameter space. To discover whether this is the case, we calculate a simple χ^2 statistic [34],

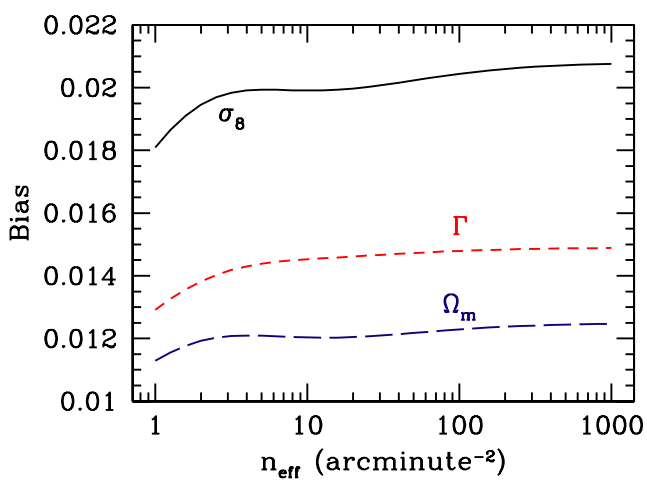

FIG. 3 (color online). The bias due to neglecting reduced shear corrections as a function of galaxy density (per square arcminute for a 1-component rms shear of 0.25) for the three cosmological parameters varied. The bias on σ_8 is negative.

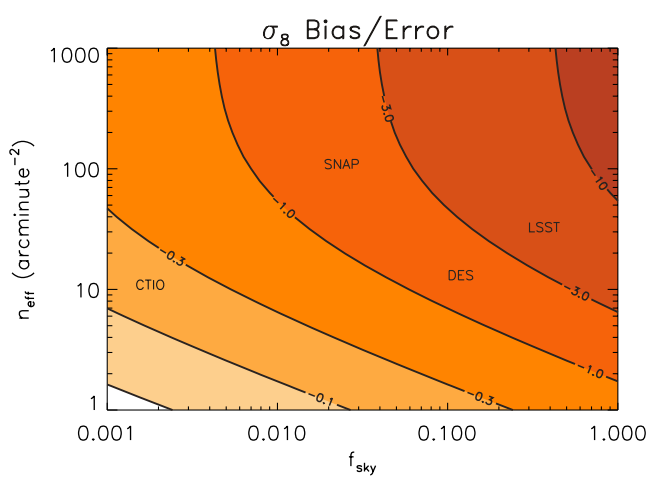

FIG. 4 (color online). The ratio of the bias on σ_8 due to neglecting reduced shear to the statistical error on σ_8. The ratio depends on the width and galaxy density of the survey. Several current and future surveys are shown for orientiation: CTIO Lensing Survey [8]; Supernova Acceleration Probe (SNAP) [39]; Dark Energy Survey (DES) [http://www.darkenergysurvey.org]; Large Scale Synaptic Survey (LSST) [40]. If the ratio is larger than 1, neglecting reduced shear corrections biases σ_8 by an amount greater than its unmarginalized statistical error.

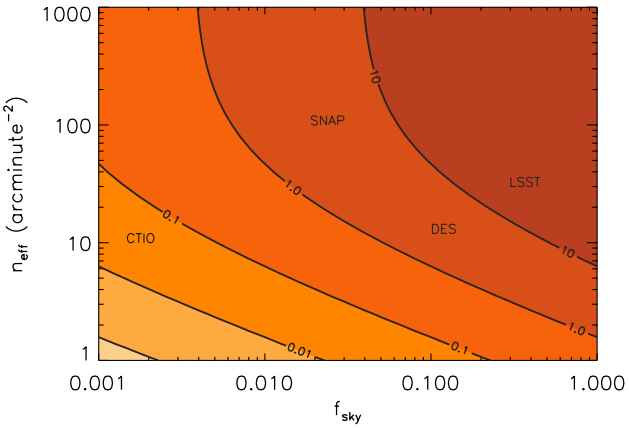

FIG. 5 (color online). Effect of reduced shear bias on the full parameter set. If $\Delta\chi^2 > 3.5$, then neglecting reduced shear will cause the correct parameter set to lie outside of the 1-σ error ellipsoid of the experiment. $\Delta\chi^2$ is shown here as a function of galaxy density and sky coverage.

$$\Delta\chi^2 = \sum_{i,j} b_i F_{ij} b_j \tag{19}$$

where $\Delta\chi^2$ is the difference in χ^2 between the biased and unbiased points in parameter space. We may then use a standard table to compute the confidence level for 3 degrees of freedom, $p(\Delta\chi^2, \nu)$, with $\nu = 3$. Figure 5 displays contours of $\Delta\chi^2$ as a function of survey width and galaxy density. LSST, for example, has $\Delta\chi^2 \approx 11 \rightarrow p \approx 0.99$. In words, if LSST does not account for reduced shear, it will rule out the correct parameter set at the 99% level. SNAP and DES will be biased at about the 1-σ level.

Both Figs. 4 and 5 illustrate that the largest of current experiments are already entering a regime in which the effects of reduced shear must be considered, and future experiments will certainly need to account for it. Note that neither of these figures accounts for priors, which can reduce errors and alter the bias, in turn magnifying the impact of reduced shear. We therefore recommend the conservative approach of using Fig. 4 as a guide to determining whether neglecting reduced shear is justified for current experiments. In that case, virtually all upcoming experiments will need to add in this correction when extracting information about cosmological parameters.

V. OTHER CORRECTIONS

Reducing the shear is not the only correction that needs to be applied to weak lensing spectra [16,19,26]. For instance, Hu and Cooray [35] have computed perturbative corrections to the power spectrum which account for the Born approximation and lens-lens coupling. These corrections are an order of magnitude smaller than the one considered here. To understand why, recall that δC_l from Eq. (9) comes from considering the product of a second order perturbation with a first order perturbation, $g^{(1)} \times g^{(2)}$. We have considered the corresponding terms for the beyond Born and lens-lens corrections and found that they vanish. Therefore, the first nonvanishing corrections are the ones considered in Ref. [35]: those of order $g^{(1)}g^{(3)}$ or $g^{(2)}g^{(2)}$. We have also not considered the effects of source clustering [36]. There is some indication [37,38] that this may also induce percent level changes in the power spectrum on small scales. If so, these would need to be included as well. Accounting for this coupling in a simulation requires input from a real 3D galaxy catalogue.

VI. CONCLUSIONS

Deflection of light rays by gravitational potentials along the line-of-sight introduces a mapping between the source and image plane. The Jacobian of this mapping defines the shear and convergence as a function of position on the sky. In the absence of size or magnification information neither the shear nor the convergence is observable, but only the combination $g = \gamma/(1 - \kappa)$, known as the reduced shear. On small scales, where lensing surveys get much of their constraining power, this must be taken into account when predicting the observables.

We have studied the difference between cosmic shear and the reduced shear. Our main conlusions are:

(i) The perturbative calculation of reduced shear, Eq. (11), agrees well with numerical simulations. This is not too surprising, since the lensing is weak and we use many components themselves fit to N-body simulations, but it gives us confidence that we can use these calculations in making predictions or fitting to data.

(ii) The effects of reduced shear are on the threshhold of becoming very relevant. As depicted in Figs. 4 and 5, upcoming surveys will need to account for reduced shear when extracting cosmological parameters.

ACKNOWLEDGMENTS

S. D. was supported by the DOE and by NASA grant NAG5-10842. M. J. W. was supported in part by NASA and the NSF. C. A. S. was supported in part by the Kavli Institute for Cosmological Physics at the University of Chicago and by grant NSF PHY-011442. The simulations were performed on the IBM-SP at NERSC.

[1] N. Kaiser, Astrophys. J. **388**, 272 (1992).
[2] Y. Mellier, Annu. Rev. Astron. Astrophys. **37**, 127 (1999).
[3] M. Bartelmann and P. Schneider, Phys. Rep. **340**, 291 (2001).
[4] S. Dodelson, *Modern Cosmology* (Academic Press, San Diego, 2003).
[5] H. Hoekstra, H. Yee, and M. Gladders, New Astron. Rev. **46**, 767 (2002).
[6] L. Van Waerbeke, Y. Mellier, and H. Hoekstra, astro-ph/0406468.
[7] C. Heymans *et al.*, Mon. Not. R. Astron. Soc. **361**, 160 (2005).
[8] M. Jarvis, B. Jain, G. Bernstein, and D. Dolney, astro-ph/0502243.
[9] K. Benabed and F. Bernardeau, Phys. Rev. D **64**, 083501 (2001).
[10] A. Refregier *et al.*, Astron. J. **127**, 3102 (2004).
[11] M. Takada and B. Jain, Mon. Not. R. Astron. Soc. **348**, 897 (2004) .
[12] A. Heavens, Mon. Not. R. Astron. Soc. **343**, 1327 (2003).
[13] W. Hu and M. Tegmark, Astrophys. J. **514**, L65 (1999).
[14] K. N. Abazajian and S. Dodelson, Phys. Rev. Lett. **91**, 041301 (2003).
[15] D. Huterer and M. Takada, Astropart. Phys. **23**, 369 (2005).
[16] P. Schneider, L. van Waerbeke, B. Jain, and G. Kruse, Mon. Not. R. Astron. Soc. **296**, 873 (1998).
[17] A. J. Barber, Mon. Not. R. Astron. Soc. **335**, 909 (2002).
[18] M. White, Astropart. Phys.**23**, 349 (2005).
[19] C. Vale and M. J. White, Astrophys. J. **592**, 699 (2003).
[20] M. J. White and C. Vale, Astropart. Phys. **22**, 19 (2004).
[21] A. J. S. Hamilton, A. Matthews, P. Kumar, and E. Lu, Astrophys. J. **374**, L1 (1991).
[22] J. A. Peacock and S. J. Dodds, Mon. Not. R. Astron. Soc. **267**, 1020 (1994).
[23] J. A. Peacock and S. J. Dodds, Mon. Not. R. Astron. Soc. **280**, L19 (1996).
[24] F. Bernardeau, S. Colombi, E. Gaztanaga, and R. Scoccimarro, Phys. Rep. **367**, 1 (2002).
[25] R. E. Smith *et al.*, (The Virgo Consortium), Mon. Not. R. Astron. Soc. **341**, 1311 (2003).
[26] B. Jain, U. Seljak, and S. D. M. White, Astrophys. J. **530**, 547 (2000).
[27] W. Hu and M. J. White, Astrophys. J. **554**, 67 (2001).
[28] S. Dodelson and P. Zhang, Phys. Rev. D **72**, 083001 (2005).
[29] P. G. Castro, Phys. Rev. D **67**, 123001 (2003).
[30] R. Scoccimarro and H. M. P. Couchman, Mon. Not. R. Astron. Soc. **325**, 1312 (2001),.
[31] H. Hoekstra, M. Franx, and K. Kuijken, astro-ph/9910487.
[32] M. White, Astropart. Phys. **22**, 211 (2004).
[33] H. Zhan and L. Knox, Astrophys. J. **616**, L75 (2004).
[34] W. H. Press, S. A. Teukolsky, W. T. Vetterling, and B. P. Flannery, *Numerical Recipes in C* (Cambridge University Press, Cambridge, 1992).
[35] A. Cooray and W. Hu, Astrophys. J. **574**, 19 (2002) .
[36] F. Bernardeau, Astron. Astrophys. **338**, 375 (1998).
[37] T. Hamana, Mon. Not. R. Astron. Soc. **326**, 326 (2001).
[38] P. Schneider, L. van Waerbeke, and Y. Mellier, Astron. Astrophys. **389**, 729 (2002).
[39] J. Albert *et al.*, (SNAP), astro-ph/0507460.
[40] J. A. Tyson, D. M. Wittman, J. F. Hennawi, and D. N. Spergel, Nucl. Phys. B, Proc. Suppl. **124**, 21 (2003).